Seizure: European Journal of Epilepsy 69 (2019) 180–185

Contents lists available at ScienceDirect

Seizure: European Journal of Epilepsy

journal homepage: www.elsevier.com/locate/seizure

Homozygous missense *TPP1* mutation associated with mild late infantile neuronal ceroid lipofuscinosis and the genotype-phenotype correlation

Zi-Rong Chen[a,b,1], De-Tian Liu[a,1], Heng Meng[c], Liu Liu[d], Wen-Jun Bian[a], Xiao-Rong Liu[a], Wei-Wen Zhu[a], Yong He[a], Jie Wang[a], Bin Tang[a], Tao Su[a], Yong-Hong Yi[a,*]

[a] Institute of Neuroscience and the Second Affiliated Hospital of Guangzhou Medical University, Key Laboratory of Neurogenetics and Channelopathies of Guangdong Province and the Ministry of Education of China, Guangzhou, Guangdong, China
[b] Department of Neurology of the First Affiliated Hospital of Guangxi Medical University, Nanning, Guangxi, China
[c] Department of Neurology of the First Affiliated Hospital of Jinan University and Clinical Neuroscience Institute of Jinan University, Guangzhou, Guangdong, China
[d] Department of Neurology, Xiaoshan First People's Hospital, Hangzhou, Zhejiang, China

ARTICLE INFO

Keywords:
TPP1
Late infantile neuronal ceroid lipofuscinosis
Destructive mutation
Genotype-phenotype correlation

ABSTRACT

Purpose: *TPP1* mutations have been identified in patients with variable phenotypes such as late infantile neuronal ceroid lipofuscinosis (LINCL), juvenile neuronal ceroid lipofuscinosis (JNCL), and spinocerebellar ataxia 7. However, the mechanism underlying phenotype variation is unknown. We screened *TPP1* mutations in patients with epilepsies and analyzed the genotype-phenotype correlation to explain the phenotypic variations.

Methods: We performed targeted next-generation sequencing in a cohort of 330 patients with epilepsies. All previously reported *TPP1* mutations were systematically retrieved from the PubMed and NCL Mutation Database.

Results: The homozygous missense *TPP1* mutation c.646 G > A/ p.Val216Met was identified in a family with two affected siblings. The proband presented with seizures from three years of age, while no ataxia, cognitive regression, or visual abnormalities were observed. Further analysis of all reported *TPP1* mutations revealed that the LINCL group had a significantly higher frequency of truncating and invariant splice-site mutations than the JNCL group. In contrast, the JNCL group had a higher frequency of variant splice-site mutations than LINCL. There was a significant correlation between phenotype severity and the frequency of destructive mutation.

Conclusion: This study suggested that the phenotype of mainly epilepsy can be included in the phenotypic spectrum of *TPP1* mutations, which are candidate targets for genetic screening in patients with epilepsy. With the development of therapy techniques, early genetic diagnosis may enable the improvement of etiology-targeted treatments. The relationship between phenotype severity and the genotype of *TPP1* mutations may help explain the phenotypic variations.

1. Introduction

TPP1 (OMIM*607,998) encodes lysosomal enzyme tripeptidyl peptidase 1 (TPP1), a member of the serine-carboxyl proteinase family. TPP1 is an aminopeptidase that releases of N-terminal tripeptides from a polypeptide and is involved in the processing of neuron-specific trophic factors [1,2]. This protein also shows minor endopeptidase activity [3]. Deficient TPP1 activity in mutant mouse models resulted in intralysosomal accumulation of autofluorescent storage materials, neuronal loss, and widespread axonal degeneration [4]. In humans, *TPP1* mutations cause late infantile neuronal ceroid lipofuscinosis (LINCL) [5,6]. The symptoms typically appear between 2 and 4 years of age with seizure onset, followed by ataxia, progressive cognitive and motor dysfunction, and visual impairment later in the disease course [7,8].

TPP1 defects are associated with not only LINCL, which is the typical phenotype, but also juvenile neuronal ceroid lipofuscinosis (JNCL), which generally has an onset age of 6–10 years with a protracted disease course [9,10]. Recently, *TPP1* mutations were identified in patients with ataxia [11–13], including spinocerebellar ataxia 7 (SCAR7) which has a later onset and more restricted phenotype without epilepsy, cognitive regression, or ophthalmologic abnormalities. These

* Corresponding author at: Institute of Neuroscience and Department of Neurology of the Second Affiliated Hospital of Guangzhou Medical University, Chang-Gang-Dong Road 250, Guangzhou, 510260, China.
E-mail address: yyh168@sina.com (Y.-H. Yi).
[1] These authors contributed equally to this work.

https://doi.org/10.1016/j.seizure.2018.08.027
Received 4 June 2018; Received in revised form 29 August 2018; Accepted 31 August 2018

phenotypes varied in severity, ranging from severe LINCL, delayed onset, and protracted JNCL, to mild SCAR7. However, the mechanism underlying phenotype variation is unknown. Previous studies showed that the residual TPP1 enzyme activity level was associated with phenotypic severity [4,14]. It remains unclear whether phenotype variation is correlated with the genotypes of *TPP1* mutations.

In this study, we performed targeted next-generation sequencing in a cohort of patients with epilepsies. A homozygous missense mutation in *TPP1* was identified in a family with two affected siblings. We further systematically reviewed all *TPP1* mutations and analyzed the correlations between genotype and phenotype.

2. Methods

2.1. Patients

The case was from a cohort of 330 patients with epilepsies in the Epilepsy Center of the Second Affiliated Hospital of Guangzhou Medical University in China. Patients in this cohort were diagnosed with epilepsies without acquired causes and were subjected to genetic testing to determine the potential etiology of epilepsy. The collected clinical data included onset age, initial symptom, main signs and symptoms, seizures types and frequency, response to antiepileptic drugs, ophthalmologic data, general and neurological examination results, and detailed family history. Developmental states were evaluated, including fine and gross motor, language, and adaptive personal/social skills. Brain magnetic resonance imaging was performed to detect brain structure abnormalities. Long-term (24 h) video-electroencephalography (EEG) monitoring records were obtained. All EEGs were reviewed by two qualified electroencephalographers.

The study was approved by the institutional review board and ethics committee of the hospital. This study adhered to the guidelines of the International Committee of Medical Journal Editors with regard to patient consent for research or participation.

2.2. Targeted sequencing and analysis

From blood samples collected from patients and their parents, genomic DNA was extracted from the peripheral blood using the Qiagen Flexi Gene DNA Kit (Qiagen, Hilden, Germany). Genetic variants were detected using a custom targeted next-generation sequencing gene panel for epilepsy genes (Supplementary Table 1).

Stepwise filtering was applied to derive potential pathogenic variants, including 1) variants with a minor allele frequency of < 0.005 in the 1000 Genomes and Exome Aggregation Consortium or variants reported in HGMD and/or OMIM databases; 2) annotation-based filtration to remove variants in segmental duplication regions prone to produce false-positive variant call due to mapping errors; and 3) variants predicted to be deleterious in sequence conservation or damaging to protein function by one or more *in silico* tools (SIFT, PolyPhen-2, and Mutation Taster). Splice-site variants with altered splicing effects by the Human Splicing Finder were included. Sanger sequencing was used to validate all candidate pathogenic variants. The pathogenicity of the variants was evaluated by the American College of Medical Genetics and Genomics, for which population data, computational data, allelic data, functional damaging, inheritance pattern, and information from other databases were considered [15]. The clinical concordance of the mutations was also assessed as we previously described [16].

2.3. Analysis of genotype-phenotype correlation

We retrieved all *TPP1* mutations (NM_000391.3) from the PubMed (http://www.ncbi.nlm.nih.gov/pubmed/) and NCL Mutation Database (http://www.ucl.ac.uk/ncl/mutation.shtml) up to February 2018. All selected CLN2 cases (288 families) were explicit in alleles. Cases with ambiguous alleles (63 families) were not included. All *TPP1* mutations were validated by direct sequencing in the original reports. To avoid duplicate recruitment, mutations were cross-referenced for their genetic and clinical information.

To facilitate analysis of the correlation between genotype and phenotype, gene mutations are classified into destructive mutations, variant splice-site mutations, and missense mutations. Destructive mutations cause gross protein malformations and lead to haploinsufficiency, including truncating mutations (nonsense and frameshifting) and invariant splice-site mutations which are mutations within 2 base pairs of the splice donor-sites or acceptor-sites [17]. Variant splice-site mutations refer to those outside of 2 base pairs of the splice site and deeper in intronic regions [17]. The phenotypes of *TPP1* mutations were classified as LINCL, JNCL, and SCAR7 according to data in the NCL Mutation Database. Furthermore, we assessed all cases previously diagnosed as LINCL and compared the onset age and evolution with the general cases [18]. Cases with slow progression or relatively later onset were considered as mild LINCL.

Statistical analyses were performed using SPSS version 21.0 (SPSS, Inc., Chicago, IL, USA). Chi-square test or Fisher's exact test was applied to compare the frequencies of mutations between different phenotype groups. The relationship between phenotype and the occurrence of destructive mutation was analyzed by Spearman's correlation test. Values of $p < 0.05$ (two-sided) were considered significant.

3. Results

3.1. Identification of TPP1 mutation

A homozygous missense mutation in *TPP1*, c.646 G > A/p.Val216Met, was identified in a family with two affected siblings. This mutation was transmitted from asymptomatic parents who were heterozygous for the same genetic defect (Fig. 1A and B). This mutation was not present in the general populations of either the 1000 Genomes Project or Exome Aggregation Consortium. In cross-species comparison, the amino acid sequence alignment of *TPP1* showed that p.Val216Met is highly conserved in various species. The pathogenicity of p.Val216Met was estimated as deleterious by web-based prediction tools. A compound heterozygosity (p.Val216Met and c.1551 + 1G > A) was identified in a patient with LINCL, which was confirmed pathologically in our previous study [19]. According to American College of Medical Genetics and Genomics standards and guidelines for the interpretation of sequence variants, p.Val216Met was estimated as a likely pathogenic variant (Fig. 1C) with clinical concordance.

3.2. Clinical features of patients with TPP1 mutation

The two patients were full-term born from healthy and non-consanguineous parents. The proband (II-1) was an 8-year-old girl who had her first seizure at 3 years of age. She presented seizures that started with deviation of the eyes to left and then loss of consciousness, which persisted for 20–30 s. The seizures recurred 4–8 times per week. Secondary generalized tonic-clonic seizure developed at the age of 5 years, and the attacks occurred approximately several times per month. Her parents complained that the patient had difficulty with running; but no ataxia, cognitive regression, or visual abnormalities were observed. The patient did not respond to valproate. Her video EEG recordings showed multifocal spikes and slow waves (Fig. 2A). Brain magnetic resonance imaging showed mild atrophy of the cerebellum (Fig. 2B).

Her younger brother had similar seizures starting at the age of 3.5 years (II-2), but without other neurological or ophthalmologic abnormalities. EEGs showed generalized discharges (Fig. 2C) and neuroimaging showed mild cerebellar atrophy (Fig. 2D).

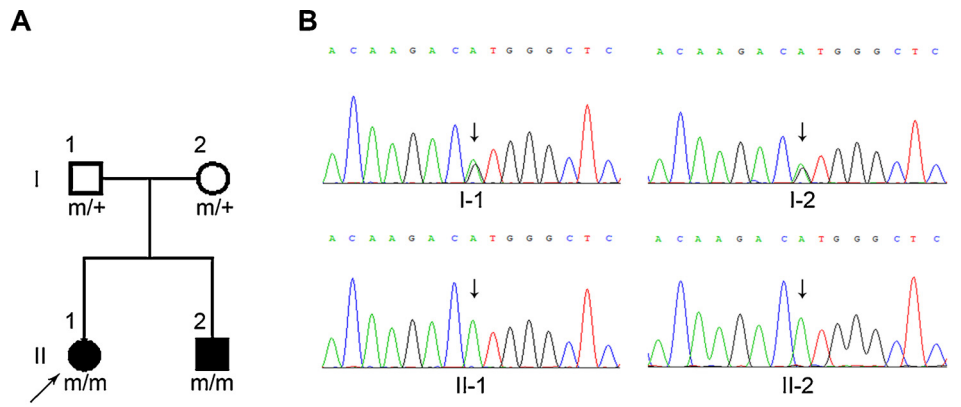

C In silico analysis and ACMG scoring of p.Val216Met

Mutation	SIFT	PP2-Var	Mutation Taster	Novel/reported /(hotspot)	MAF-KG	MAF-ExAC	ACMG Scoring	ACMG pathogenicity
p.Val216Met	Damaging	Probably damaging	Disease causing	Reported	None	None	PM2+PM3+PP1 +PP3+PP4	Likely pathogenic

Fig. 1. Pedigree and mutation of the family with *TPP1* mutation. A The pedigree of the family. The parents were asymptomatic. Individuals carrying one mutation and one normal allele are denoted by m/+, whereas the one with two mutations by m/m. B Sequencing chromatogram for c.646 G > A/ p.Val216Met. Arrow indicates the variant allele. **C** *In silico* analysis and American College of Medical Genetics and Genomics (ACMG) scoring of mutations. ExAC: Exome Aggregation Consortium; KG: 1000 Genomes Project; MAF: Minor Allele Frequency; PP2: PolyPhen-2; PM2: absent in population databases; PM3: for recessive disorders, detected in trans with a pathogenic variant; PP1: cosegregation with disease in multiple affected family members; PP3: multiple lines of computational evidence support a deleterious effect on the gene /gene product; PP4: patient's phenotype or family history highly specific for gene; SIFT: Sorts Intolerant From Tolerant.

3.3. Genotype-phenotype correlation

To determine the whole phenotypic spectrum and possible genotype-phenotype correlation, we systematically reviewed all *TPP1* mutations and their associated phenotypes. To date, 126 *TPP1* homozygous or compound heterozygous mutations have been identified in 288 unrelated cases (Supplementary Table 2). The mutation-associated phenotypes included LINCL (n = 175, 60.8%), JNCL (n = 15, 5.2%), SCAR7 (n = 3, 1.0%), and unclassified cases (n = 95, 33.0%). In the LINCL group, truncating mutations contributed to 37.4% (131/350) of cases, followed by invariant splice-site mutations (111/350, 31.7%) and missense mutations (95/350, 28.3%). Variant splice-site mutations occurred in only 0.9% (3/350) of cases (Fig. 3A). In the JNCL group, missense and variant splice-site mutations were frequent, detected in 43.3% (13/30) and 30% (9/30) of cases, respectively (Fig. 3B). The LINCL group had a significantly higher frequency of truncating and invariant splice-site mutations than the JNCL group ($p = 0.023$ and $p = 0.004$, respectively). In contrast, the JNCL group showed a significantly higher frequency of variant splice-site mutations than the LINCL group ($p < 0.001$). Three cases of SCAR7 have been reported, all of which were compound heterozygotes, in which one allele was an invariant splice-site mutation and the others were missense mutations. The SCAR7 group was not included in statistical analysis because of the limited number of cases.

In the present study, the two patients carried homozygous missense mutations and presented a mild clinical phenotype with a relatively protracted illness course. To explore the potential genetic basis of the disease, we searched for publications of similar mild cases in the LINCL group. Five cases with mild phenotypes were identified (Table 1) and presented slow progression or relatively later onset [20–22]. We compared the genotypes of the classic LINCL group with those of the mild LINCL group. Mild LINCL cases showed a lower allele frequency of destructive mutation than those with classic LINCL (60.0% vs 68.5%), but no significant difference was detected between the two groups. In contrast, Spearman's correlation test revealed a significant correlation between the frequency of destructive mutation and phenotype severity ($p < 0.001$, Fig. 4), which included classic LINCL, mild LINCL, and JNCL.

4. Discussion

In the present study, we identified a homozygous missense *TPP1* mutation (c.646 G > A/ p.Val216Met) in a family with two affected siblings with epilepsy. This case was from a cohort of 330 patients with epilepsies, and patients with *TPP1* mutations mainly presented epilepsy with protracted evolution. This finding suggests that *TPP1* is a candidate target for genetic screening in patients with epilepsy. Further analysis revealed a potential correlation between phenotype and genotype, providing insight into the mechanism of phenotypic variations of *TPP1* mutations.

Currently, *TPP1* mutations have been reported to be associated with LINCL (60.8%), JNCL (5.2%), and SCAR7 (1.0%). All patients with *TPP1* mutations were homozygous or compound heterozygous mutations. In patients with LINCL, most mutations were destructive, including truncating and invariant splice-site mutations that mainly lead to complete TPP1 functional deficiency and haploinsufficiency. LINCL is the most common phenotype associated with *TPP1* mutations. Seizures or ataxia typically occur in the early stage of disease, followed by progressive loss of motor functions and cognitive decline. Visual abnormality develops later in the disease course, and death typically occurs in the second decade [23]. In contrast, in patients with JNCL, missense and variant splice-site mutations were most common. JNCL presents in children at 5–10 years of age with a progressive loss of vision, epilepsy, dementia, and motor disturbances followed by a protracted disease course and typically death in the middle of the third decade of life [24]. Previous studies showed that the variable phenotypes likely depend on the functional impact of *TPP1* mutations, which caused complete or partial TPP1 deficiencies [25–27] that were correlated with neuronal loss in subpopulations of the brain [28]. It is generally considered that mutations abolishing TPP1 enzyme activity lead to LINCL, whereas mutations partially affecting TPP1 enzyme activity may lead to mild and protracted phenotypes. Missense mutations vary in residual TPP1 activity and mutants with variant splice-site mutations produce aberrant and normal transcripts [29], explaining the mild phenotype of JNCL. The present study demonstrated a correlation between the genotype of *TPP1* mutations and phenotype severity, indicating the significance of genotype evaluation in the diagnosis and outcome prediction in clinical practice and genetic counseling.

In the present study, a homozygous missense *TPP1* mutation was identified in two affected siblings. The patients showed seizure onset at

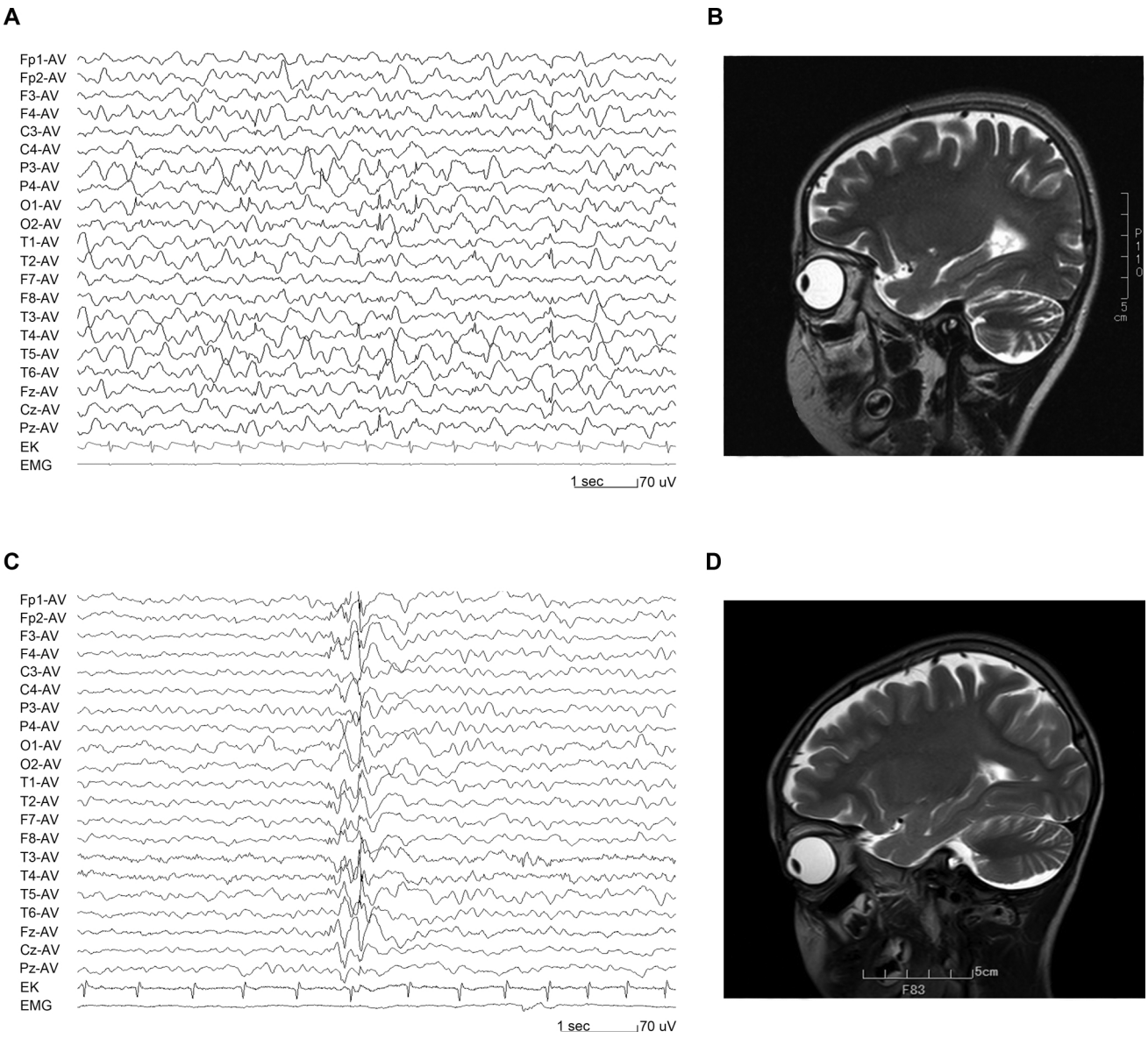

Fig. 2. EEG and MRI changes in the patients with *TPP1* mutation. A EEG of the proband (II-1) shows slow waves and multifocal discharges. B MRI of the proband (II-1) shows mild atrophy of cerebellum (Sagittal T2-weight). C EEG of patient (II-2) shows generalized discharges. D MRI of patient (II-2) shows mild cerebellum atrophy.

the typical age in LINCL, but without apparent neurodevelopmental regression as classical LINCL. In patients with classic LINCL, seizure typically appears at the end of the third year of life, motor function progress with a rapid decline at approximately the age of five years, and the average onset age of visual symptoms is four years [18]. Currently, 59 *TPP1* missense mutations have been identified and formed homozygous or compound heterozygous mutations in patients with variable severity (http://www.ucl.ac.uk/ncl/mutation.shtml). Previously, p.Arg447His with variable mutations in compound heterozygosity have been identified in cases with milder and protracted phenotypes [20,21,30,31], suggesting milder functional impairment caused by this missense mutation. In contrast, a recent study identified the homozygous missense mutation p.Asp276Val, which disrupts enzyme activity and causes a severe phenotype with early onset [9]. The proband in this study carried the homozygous missense mutation p.Val216Met and presented slowly progressive evolution without other obvious clinical symptoms except for epilepsy. These findings suggest that missense mutations are associated with phenotypes of variable severities, which may be determined by the functional defect caused by the mutations. Similarly, splice-site mutations at different depths in the intron were associated with variable functional defects [17]. Further studies are required to examine the functional deficiency of *TPP1* missense and splice-site mutations and their correlations with phenotype.

Notably, C.509-1G > C and p.Arg208* are hot spot mutations that mostly cause classic CLN2. However, they also were associated with mild phenotypes in rare cases. The mechanisms underlying such phenotypic variations are unknown. A recent study suggested that complex networks of genetic interactions underlying traits and background modifiers, among many other factors, explain the phenotype [32].

This study suggested that the phenotype of mainly epilepsy can be included in the phenotypic spectrum of *TPP1* mutations. Previously, *TPP1* mutations p.Gln278Arg and p.Gln422His were identified in a cohort of 33 index patients with concise epilepsy phenotypes or with a severe but unspecific seizure disorder by using a panel of 265 genes [33]. This result suggested that *TPP1* mutations are candidate targets for genetic screening in patients with epilepsy. Recent studies revealed that several approaches, such as gene therapy and enzyme replacement, are promising therapeutic strategies for LINCL. With the development

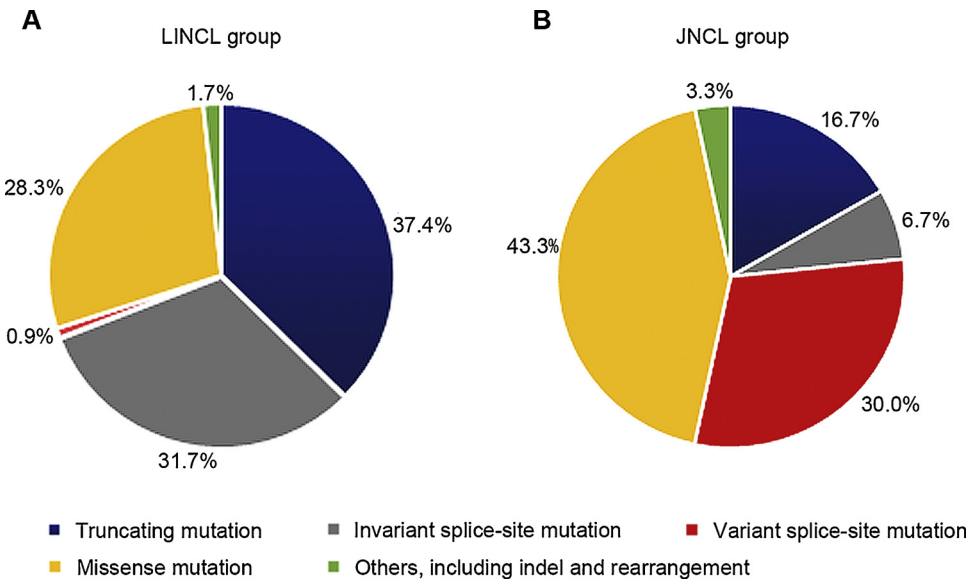

Fig. 3. Overview of genotype distribution of *TPP1* mutations. A Genotypes of *TPP1* mutation in late infantile neuronal ceroid lipofuscinosis (LINCL) group. Allele frequencies of *TPP1* mutations in LINCL group demonstrate a predominance of truncating mutations (37.4%) and invariant splice-site mutations (31.7%). B Genotypes of *TPP1* mutation in juvenile neuronal ceroid lipofuscinosis (JNCL) group. JNCL group had a higher frequency of variant splice-site mutation than LINCL (30% vs 0.9%, $p = 0.007$).

of therapy techniques, early genetic diagnosis may improve patient conditions with the etiology-targeted treatments.

In conclusion, we identified a novel homozygous missense *TPP1* genotype in two siblings with mild and protracted LINCL. This finding may extend the phenotypic spectrum of *TPP1* mutations. Systematic analysis of *TPP1* mutations revealed correlations between genotype and phenotype severity, which help explain the phenotypic variation.

Conflicts of interest

The authors declare that they have no conflict of interest.

Acknowledgements

This work was supported by the National Natural Science Foundation of China (Grant Nos. 81571273, 81471149, and 81501125), and Science and Technology Project of Guangzhou (Grant Nos. 201604020161 and 201607010002).

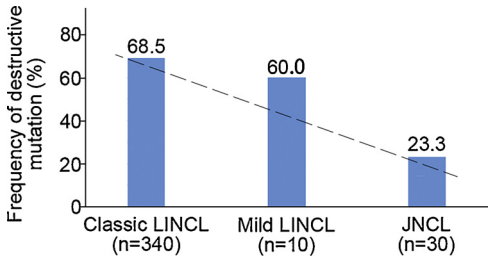

Fig. 4. The frequencies of destructive *TPP1* mutation in classic LINCL group, mild LINCL group, and JNCL group. The values are expressed as the percentage of alleles as destructive mutations in each group. Spearman's correlation test was used for the correlation analysis and indicated a significant correlation between the frequency of destructive mutation and the phenotype severity ($p < 0.001$).

Table 1
Variable phenotypes of *TPP1* mutations.

Allele 1	Allele 2	Onset(y)	Seizure	Ocular	pyramidal	Cerebellar	Behavior	Cognitive	Reference
Mild LINCL									
c.509-1G > A	c.509-1G > C	3.5	+	+	+	+	–	+	[22]
p.Arg208*	p.Arg208*	3	+	–	–	+	–	+	[21]
p.Val216Met	p.Val216Met	3-3.5	+	–	–	+	–	–	present
p.Arg447His	p. c.509-1G > C	6-8	+	+	–	+	+	+	[21]
p.Arg447His	p.Gln264*	6-9	–	–	+	+	–	+	[20]
JNCL									
c.509-1G > A	5' rearrangement	7	–	+	–	–	+	–	[22]
c.887-10A > G	c.887-10A > G	10	+	–	–	–	–	+	[10]
p.Gln66*	c.887-10A > G	9	+	+	+	+	–	+	[9]
p.Arg208*	c.887-10A > G	5-9	n. a.	n. a.	n. a.	n. a.	n. a.	n. a.	[30]
p.Asp276Val	c.887-10A > G	10	n. a.	n. a.	n. a.	n. a.	n. a.	n. a.	[30]
p.Arg350Trp	p.Gly535Arg	4-5	n. a.	n. a.	n. a.	n. a.	n. a.	n. a.	[30]
p.Arg447His	p.Ser475Leu	5	n. a.	n. a.	n. a.	n. a.	n. a.	n. a.	[30]
p.Arg447His	c.509-1G > C	7	+	+	–	+	+	+	[31]
p.Arg447His	p.Arg208*	8	+	+	–	+	+	+	[21]
p.Ala453Val	c.89 + 5G > C	2.5-3	n. a.	n. a.	n. a.	n. a.	n. a.	n. a.	[30]
p.Ser475Leu	c.887-10A > G	3	n. a.	n. a.	n. a.	n. a.	n. a.	n. a.	[30]
p.Val480Gly	p.Arg208*	6	–	–	+	+	+	+	[28]
SCAR7									
c.509-1G > A	p.Val466Gly	18y	–	–	–	+	–	–	[12]
c.509-1G > C	p.Glu343 Asp	4y	–	–	–	+	–	–	[11]

LINCL: late infantile neuronal ceroid lipofuscinosis; JNCL: juvenile neuronal ceroid lipofuscinosis; SCAR7: spinocerebellar ataxia type 7; n. a: not available.

Appendix A. Supplementary data

Supplementary data associated with this article can be found, in the online version, at https://doi.org/10.1016/j.seizure.2018.08.027.

References

[1] Ezaki J, Takeda-Ezaki M, Oda K, Kominami E. Characterization of endopeptidase activity of tripeptidyl peptidase-I/CLN2 protein which is deficient in classical late infantile neuronal ceroid lipofuscinosis. Biochem Biophys Res Commun 2000;268:904–8.

[2] Sleat DE, Donnelly RJ, Lackland H, Liu CG, Sohar I, Pullarkat RK, et al. Association of mutations in a lysosomal protein with classical late-infantile neuronal ceroid lipofuscinosis. Science 1997;277:1802–5.

[3] Golabek AA, Kida E. Tripeptidyl-peptidase I in health and disease. Biol Chem 2006:387.

[4] Sleat DE, El-Banna M, Sohar I, Kim K, Dobrenis K, et al. Residual levels of tripeptidyl-peptidase I activity dramatically ameliorate disease in late-infantile neuronal ceroid lipofuscinosis. Mol Genet Metab 2008;94:222–33.

[5] Mole SE, Cotman SL. Genetics of the neuronal ceroid lipofuscinoses (Batten disease). Biochim et Biophys Acta (BBA) Mol Basis Dis 2015;1852:2237–41.

[6] Goldberg-Stern H, Halevi A, Marom D, Straussberg R, Mimouni-Bloch A. Late infantile neuronal ceroid lipofuscinosis: a new mutation in Arabs. Pediatr Neurol 2009;41:297–300.

[7] Perez-Poyato MS, Marfa MP, Abizanda IF, Rodriguez-Revenga L, et al. Late infantile neuronal ceroid lipofuscinosis: mutations in the CLN2 gene and clinical course in Spanish patients. J Child Neurol 2013;28:470–8.

[8] Schulz A, Kohlschütter A, Mink J, Simonati A, Williams R. NCL diseases –clinical perspectives. Biochim et Biophys Acta (BBA) Mol Basis Dis 2013;1832:1801–6.

[9] Kohan R, Cismondi IA, Dodelson Kremer R, Muller VJ, Guelbert N, et al. An integrated strategy for the diagnosis of neuronal ceroid lipofuscinosis types 1 (CLN1) and 2 (CLN2) in eleven Latin American patients. Clin Genet 2009;76:372–82.

[10] Bessa C, Teixeira CA, Dias A, Alves M, Rocha S, Lacerda L, et al. CLN2/TPP1 deficiency: the novel mutation IVS7-10A&G causes intron retention and is associated with a mild disease phenotype. Mol Genet Metab 2008;93:66–73.

[11] Dy ME, Sims KB, Friedman J. TPP1 deficiency: rare cause of isolated childhood-onset progressive ataxia. Neurology 2015;85:1259–61.

[12] Sun Y, Almomani R, Breedveld GJ, Santen GW, Aten E, Lefeber DJ, et al. Autosomal recessive spinocerebellar ataxia 7 (SCAR7) is caused by variants in TPP1, the gene involved in classic late-infantile neuronal ceroid lipofuscinosis 2 disease (CLN2 disease). Hum Mutat 2013;34:706–13.

[13] Breedveld GJ, van Wetten B, Te RG, Brusse E, et al. A new locus for a childhood onset, slowly progressive autosomal recessive spinocerebellar ataxia maps to chromosome 11p15. J Med Genet 2004;41:858–66.

[14] Katz ML, Johnson GC, Leach SB, Williamson BG, Coates JR, Whiting R, et al. Extraneuronal pathology in a canine model of CLN2 neuronal ceroid lipofuscinosis after intracerebroventricular gene therapy that delays neurological disease progression. Gene Ther 2017;24:215–23.

[15] Richards S, Aziz N, Bale S, Bick D, Das S, et al. Standards and guidelines for the interpretation of sequence variants: a joint consensus recommendation of the American College of Medical Genetics and Genomics and the Association for Molecular Pathology. Genet Med 2015;17:405–23.

[16] Zhou P, He N, Zhang JW, Lin ZJ, Wang J, Yan LM, et al. Novel mutations and phenotypes of epilepsy-associated genes in epileptic encephalopathies. Genes Brain Behav 2018:e12456.

[17] Nissim-Rafinia M, Kerem B. Splicing regulation as a potential genetic modifier. Trends Genet 2002;18:123–7.

[18] Steinfeld R, Heim P, von Gregory H, Meyer K, Ullrich K, Goebel HH, et al. Late infantile neuronal ceroid lipofuscinosis: quantitative description of the clinical course in patients with CLN2 mutations. Am J Med Genet 2002;112:347–54.

[19] Wang Y, Zeng Z, Song X, Hao Z, Shi Y, Tang B, et al. A novel CLN2/TPP1 mutation in a Chinese patient with late infantile neuronal ceroid lipofuscinosis. Neurogenetics 2011;12:93–5.

[20] Di Giacopo R, Cianetti L, Caputo V, La Torraca I, et al. Protracted late infantile ceroid lipofuscinosis due to TPP1 mutations: Clinical, molecular and biochemical characterization in three sibs. J Neurol Sci 2015;356:65–71.

[21] Wisniewski KE, Kaczmarski A, Kida E, Connell F, Kaczmarski W, Michalewski MP, et al. Reevaluation of neuronal ceroid lipofuscinoses: atypical juvenile onset may be the result of CLN2 mutations. Mol Genet Metab 1999;66:248–52.

[22] Hartikainen JM, Ju W, Wisniewski KE, Moroziewicz DN, Kaczmarski AL, McLendon L, et al. Late infantile neuronal ceroid lipofuscinosis is due to splicing mutations in the CLN2 gene. Mol Genet Metab 1999;67:162–8.

[23] Worgall S, Kekatpure MV, Heier L, Ballon D, Dyke JP, Shungu D, et al. Neurological deterioration in late infantile neuronal ceroid lipofuscinosis. Neurology 2007;69:521–35.

[24] Bennett MJ, Rakheja D. The neuronal ceroid-lipofuscinoses. Dev Disabil Res Rev 2013;17:254–9.

[25] Kousi M, Lehesjoki A, Mole SE. Update of the mutation spectrum and clinical correlations of over 360 mutations in eight genes that underlie the neuronal ceroid lipofuscinoses. Hum Mutat 2012;33:42–63.

[26] Walus M, Kida E, Golabek AA. Functional consequences and rescue potential of pathogenic missense mutations in tripeptidyl peptidase I. Hum Mutat 2010;31:710–21.

[27] Mole SE, Williams RE, Goebel HH. Correlations between genotype, ultrastructural morphology and clinical phenotype in the neuronal ceroid lipofuscinoses. Neurogenetics 2005;6:107–26.

[28] Elleder M, Dvořáková L, Stolnaja L, Vlášková H, Hůlková H, Druga R, et al. Atypical CLN2 with later onset and prolonged course: a neuropathologic study showing different sensitivity of neuronal subpopulations to TPP1 deficiency. Acta Neuropathol 2008;116:119–24.

[29] Chang EH, Zabner J. Precision genomic medicine in cystic fibrosis. Clin Transl Sci 2015;8:606–10.

[30] Kohan R, Carabelos MN, Xin W, Sims K, Guelbert N, Cismondi IA, et al. Neuronal ceroid lipofuscinosis type CLN2: a new rationale for the construction of phenotypic subgroups based on a survey of 25 cases in South America. Gene 2013;516:114–21.

[31] Sleat DE, Gin RM, Sohar I, Wisniewski K, Sklower-Brooks S, et al. Mutational Analysis of the defective protease in classic late-infantile neuronal ceroid lipofuscinosis, a neurodegenerative lysosomal storage disorder. Am J Hum Genet 1999;64:1511–23.

[32] Hou J, van Leeuwen J, Andrews BJ, Boone C. Genetic network complexity shapes background-dependent phenotypic expression. Trends Genet 2018;34:578–86.

[33] Lemke JR, Riesch E, Scheurenbrand T, Schubach M, Wilhelm C, Steiner I, et al. Targeted next generation sequencing as a diagnostic tool in epileptic disorders. Epilepsia 2012;53:1387–98.